Effect of structure transition on solidification: 'Sn-50wt%Sb' visited

Ming-Yi Xie[a]; Xian-Fen Li[a]; Cheng-Min Hu[a]; Jie Chen[a]; Lan-Jun Liu[a]; Yan-Fa Han[a]

[a] Liquid/Solid Metal Processing Institute, School of Materials Science & Engineering, Hefei University of Technology, Hefei 230009, People's Republic of China

PLEASE SCROLL DOWN FOR ARTICLE

Taylor & Francis
Taylor & Francis Group

Effect of structure transition on solidification: 'Sn–50wt%Sb' visited

Ming-Yi Xie*, Xian-Fen Li, Cheng-Min Hu, Jie Chen,
Lan-Jun Liu and Yan-Fa Han

*Liquid/Solid Metal Processing Institute, School of Materials Science & Engineering,
Hefei University of Technology, Hefei 230009, People's Republic of China*

D.C. four-probe method was used to investigate the temperature dependence of electrical resistivity of Sn–50wt%Sb melt. Anomalous changes observed on resistivity–temperature curves (ρ–T) suggest that temperature induced liquid–liquid structure transition (L-LST) might occur in Sn–50wt%Sb melt at hundreds of degrees above its liquidus, and the transition is reversible after the first heating cycle. An isothermal experiment based on ρ–T curve was conducted to further probe the effect of the L-LST on solidification morphologies. Results show that the size of the primary phase decreases and that the microstructure becomes finer when solidified from the melt experienced the irreversible L-LST.

Keywords: electrical resistivity; L-LST; solidification microstructure; Sn–50wt%Sb alloy

1. Introduction

In recent years, liquid–liquid structure transition (L-LST) has been approached by different experimental methods and theoretical calculations. It has been reported that anomalous variations of physical properties with temperature or pressure in materials reflect their structure transition. As a result, a large amount of research based on measuring physical properties such as resistivity, internal friction and heat capacity has been carried out to explore the intrinsic reason of the phenomena in liquid alloys. In previous studies, the abnormal behaviour of resistivity in different binary liquid alloys was investigated and the results indicated that L-LST took place in liquid In–Sn, Pb–Sn, Al–Cu and In–Sb alloys [1–5]. In this article, Sn–50wt%Sb was visited to probe into the effect of structure transition on solidification.

It is noticeable that Sn–Sb-based alloys have emerged as serious candidates in the search for lead-free solders in modern electronics industry. As Babbitt alloys, Sn–Sb peritectic alloys are very useful in the metallurgical field, for instance as components in bearings, and as cathode materials for use in lithium ion batteries.

In this article, the electrical resistivity of liquid Sn–50wt%Sb alloy is investigated in two continuous heating and cooling cycles, and nonlinear changes of ρ–T curves were observed in all heating and cooling cycles. In the isothermal experiment,

*Corresponding author. Email: xiemingyi2008@163.com

abnormal change also emerges in the curve of resistivity–time (ρ–t) when the melt was held at $750°C$ for 240 min. The abrupt change of resistivity with temperature or time suggests that L-LST took place in Sn–50wt%Sb melt. In the following procedure, solidification experiment was conducted to investigate the effect of irreversible L-LST on solidification morphologies.

2. Experimental procedure

Electrical resistivity measurement of Sn–50wt%Sb was carried out by D.C. four-probe method and the value was recorded continuously in several heating and cooling cycles. Weighted amounts of 99.99% pure tin and antimony granules, covered with B_2O_3, were melted and held at the temperature of $600°C$ in a ceramic crucible in resistance furnace for 40 min. Then the melts were poured into quartz cells for resistivity experiments in purified argon media (5N). The voltage drops were recorded by a Keithley-2182 nanovoltmeter, and the constant current of 500 mA was supplied by the PF66M sourcemeter. Both the heating and cooling rates were set as $5°C\,min^{-1}$. According to the temperature range of the abnormal changes on ρ–T curve, the isothermal experiment was set as that Sn–50wt%Sb melt was held at $750°C$ and resistivity versus time (ρ–t) curve was collected.

Based on the result of isothermal experiment, $750°C$ was set as melting and holding temperature in the solidification experiments. A pair of samples (A and B), with identical composition and weight (20 g), were prepared for Sn–Sb50wt% alloys. Then they were melted and held at $750°C$ for 240 and 340 min, respectively, in assigned ceramic crucibles. Both samples were covered with B_2O_3 to prevent from volatilisation and oxidation during the whole experiments process. After being held for the set time, the two samples were poured into a metal mould for solidification.

3. Results and discussion

Figure 1 shows the ρ–T curves of the liquid Sb–50wt%Sb alloy in two continuous heating and cooling cycles. It should be noted that, with the purpose to avoid the overlapping of curves, the ordinate values of all ρ–T curves were plus or minus certain values in all cycles except the second heating process. It can be seen that the electrical resistivity of liquid Sn–50wt%Sb alloy obviously changes within certain temperature range in all cycles. Both the heating and cooling turning points are hundreds of degrees above the liquidus and the turning temperature difference between heating and cooling is due to the transition hysteresis which arises from the dynamic effects. Similar phenomena are found in Bi–Sb alloys [5]. Since resistivity is one of the physical properties sensitive to structures [6], the abnormal changes of ρ–T curve suggest that L-LST probably occurs in Sn–50wt%Sb melts. Moreover, two sorts of transitions took place: the one in the first heating cycle being irreversible, and the one in second cooling and heating cycles being reversible.

It is accepted that atomic bonds of crystals are only partly broken on melting, and some amounts of short-range orders with corresponding crystal structure are still remaining in liquids [7–9]. It was reported that the coordination number of Sb increases from three in crystalline state to 4.6–8.7 in liquid state, which reflects that a
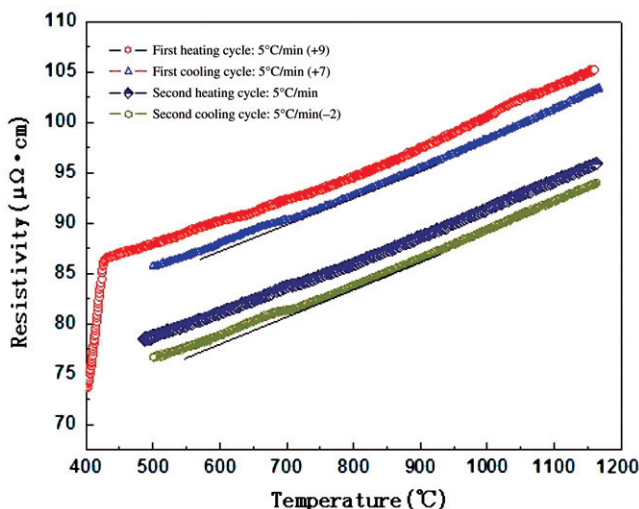
Figure 1. The resistivity–temperature curves of Sn–50 wt%Sb alloy in two heating and cooling cycles.

semi-metal to metal transformation takes place in the process of melting. Moreover, it is proved experimentally and theoretically that a clear shoulder appears on the high-Q side of the first peak of S(Q) of liquid Sb at 660°C and disappears at 800°C [10]. The results mentioned above suggest that some metastable $(Sb)_n$ short-range orders (SROs) with covalent characteristic is steady at low temperatures, gradually transform into stable SROs with temperature increasing. It might be reasonable to suggest that some amounts of similar metastable SROs (such as Sn–Sn SROs, Sb–Sn SROs, $(Sb)_n$ SROs) exist in liquid Sn–Sb alloys at a low temperature, then these metastable SROs are broken continuously as enough energy is gained to overcome the energy barrier with temperature rising until a stable state, i.e. new homogeneous liquid structure builds up. This metastable to stable transition in liquid Sn–Sb alloys is irreversible, which results in the different character of ρ–T curve between first heating cycle and that of the subsequent cycles. It means that the liquid state after melting is not in equilibrium and the long-range diffusion and nanoclusters nucleation processes should occur to reach the equilibrium.

According to the results of neutron scattering experiments [11], there is a clear shoulder on the high-Q side of the first peak of S(Q) at 300°C and 500°C, and even at 1600°C, such a shoulder may still be present. As we know, the shoulder is the sign of a covalent bond. These features for liquid Sn indicate that some tetrahedral SROs with covalent characteristics may remain in liquid Sn at lower temperature, and at least the fragments of tetrahedral unit may persist even at high temperatures in liquid Sn [12]. Based on the result of neutron scattering experiments, we can postulate that the tetrahedral SROs with covalent characteristic in liquid Sn–Sb melts may be the main cause of the reversibility of L-LST.

As discussed above, we presume that a stable state of liquid Sn–Sb alloys is built up and new liquid structure is formed after the first heating cycle. The stable liquid may contain some SROs with a reversible change character, and that kind of change can present reversible performance on ρ–T curves on heating and cooling cycles.

According to Figure 2, an abnormal change can be observed when holding Sn–50wt%Sb melt at 750°C for 240 min, which reflects that irreversible L-LST takes place during isothermal process. Through the tangent method, t_s(240 min) and t_e(340 min) were set as the beginning and ending time of the transition. Based on the results of Sn–50wt%Sb isothermal experiments, corresponding solidification experiments were designed in order to probe into the effect of irreversible L-LST on solidification. The metallograph of Sn–50wt%Sb solidified from different melt state are shown in Figure 3. Sample A is solidified from the melt before irreversible L-LST (held at 750°C for 240 min), and sample B from the melt after irreversible
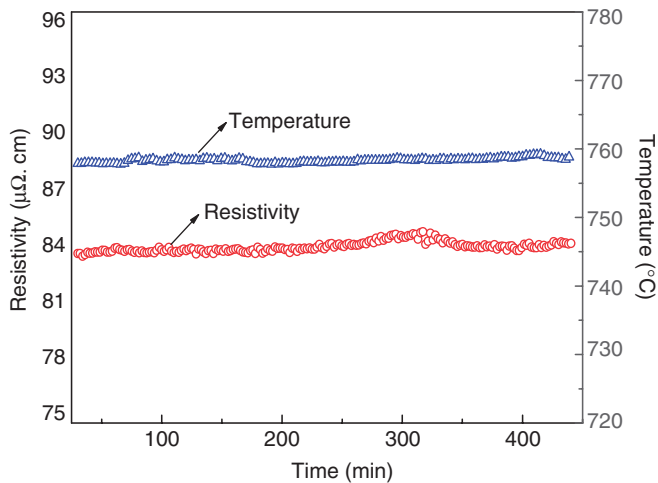

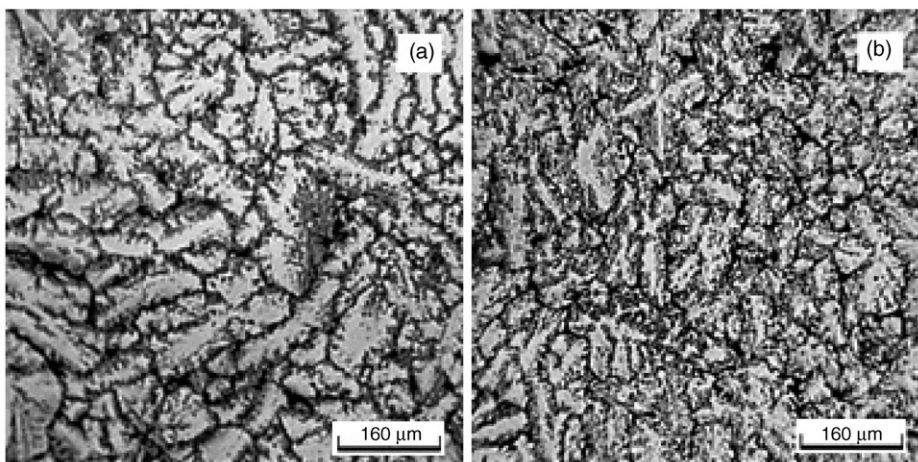Figure 2. Resistivity–time curves of Sn–50 wt%Sb at 750°C.

Figure 3. Solidification microstructures of Sn–50 wt%Sb held at 750°C for (a) 240 min and (b) 340 min.

L-LST (held at 750°C for 340 min). Both sample A and sample B were cooled down from 750°C at the same cooling rate.

As seen in Sn–Sb equilibrium phase diagram (Figure 4) [13], the Sn–50wt%Sb composition alloy β phase begins to precipitate when the melt is cooled below 423°C (liquidus), and finally single β phase is obtained at room temperature under equilibrium condition. In fact, it is far from the equilibrium state when the melt is cast into steel mould. Figure 3 shows the morphology of the phases in sample A and
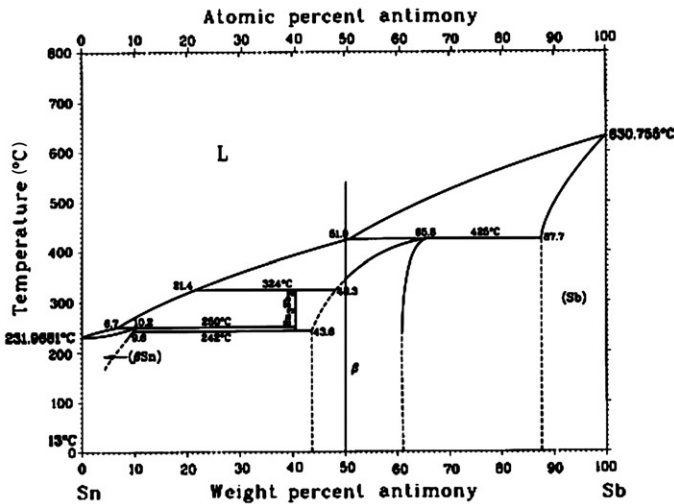
Figure 4. Sn–Sb equilibrium phase diagram.
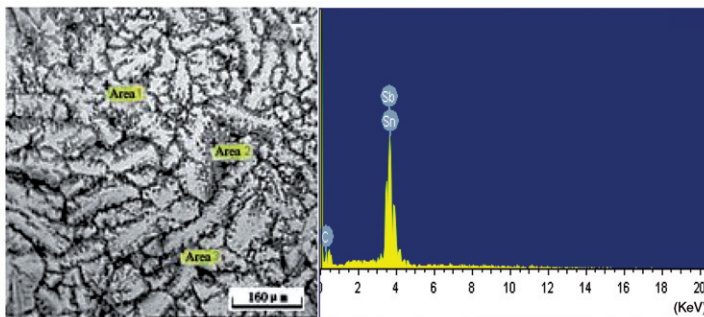
	Element	wt %	Atom%	
Area 1	Sn	38.94	39.55	β_1 (Sn$_2$Sb$_3$)
	Sb	61.06	60.45	
Area 2	Sn	43.17	43.80	β_2 (Sn$_{43}$Sb$_{57}$)
	Sb	56.83	56.20	
Area 3	Sn	51.72	52.36	β_3 (Sn$_{52}$Sb$_{48}$)
	Sb	48.28	47.64	

Figure 5. Energy dispersive X-ray of Sn–50 wt%Sb alloy.

sample B, three distinct areas can be observed: white area, grey area and dark area. Energy dispersive X-ray spectrum (EDS) was adopted to distinguish the composition of the three areas; and the result (as shown in Figure 5) confirmed that: white area is Sn_2Sb_3 (β_1); grey area is $Sn_{52}Sb_{48}$ (β_3), and $Sn_{43}Sb_{57}$ (β_2) was detected in the fringe of β_1. As discussed in [14], β_1, β_2 and β_3 all belong to β phase. The dark area is very small and it is distributed among β phase so it is hard to be distinguished from β by EDS. For the mounts of β_1 is much more than β_2 and β_3, it is reasonable to infer that the dark area is β(Sn), which has been proved to be present in Sn–80wt%Sb with similar solidification condition by X-ray diffraction in our previous study.

During the nonequilibrium solidification process, when the melt is cooled below 423°C (liquidus), primary phase β_1 begins to precipitate, then β_2 and β_3 in order. With temperature decreased to 324°C, there will remain much residual liquid, the solidification reaction might be described as following [15]: $L + \beta \longrightarrow Sn_3Sb_2$, Sn_3Sb_2 is an unstable phase which disassembles at about 242°C, $Sn_3Sb_2 \rightarrow \beta(Sn) + \beta$. In our previous study, the intermediate phase Sn_3Sb_2 was detected by quenching at 275°C after the melt of Sn–42wt%Sb was held for 3 h, which confirmed that the peritectic reaction exists.

Compared with Figure 3(a), it is apparent that the microstructure is much finer in Figure 3(b), which solidified from the liquid experienced irreversible L-LST, and average number of grain in area unit (several 1 mm^2 area) is calculated. The grain number of sample A is 187, while B is 264, so the sample B is evidently finer than sample A. The amount of primary phase (β_1: Sn_2Sb_3) in sample B is less than that of sample A as indicated by calculations using the Image-pro plus software.

From the analysis of irreversible resistivity both in the first heating cycle and in the isothermal experiment, it can be suggested that an irreversible liquid–liquid structure transition occurs in Sn–50wt%Sb alloys at temperatures of hundreds of degrees above corresponding liquidus. The intrinsic reason of the phenomenon might be explained that some metastable SROs have been broken up when held at 750°C for 340 min, thus melted alloys become more homogeneous and stable. According to the relation between critical radius and undercooling in classical nucleation theory, the smaller and disordered clusters could not grow to the size of critical size, unless at a greater undercooling. However, nucleation rate will increase promptly once the required critical undercooling was met and abundant primary phase will precipitate in sample B, thus more uniform and finer morphologies of microstructure would form on solidifying.

4. Conclusions

In summary, measurements of the electrical resistivity of Sn–50wt%Sb and analysis of ρ–T and ρ–t curves suggest that L-LST takes place in Sn–50wt%Sb melt. Two sorts of structure transitions occur in the melt, irreversible in the first heating cycle and reversible in the subsequent cycles.

The results of solidification experiments reflect that the irreversible L-LST has great effect on the solidified microstructure, namely, the size of primary phase decreases and the microstructure becomes finer when the sample is solidified from the melt experiencing irreversible L-LST.

Acknowledgements

References

[1] F.Q. Zu, L.J. Guo, Z.G. Zhu, and Y. Feng, Chin. Phys. Lett. **19**, 94 (2002).

[2] F.Q. Zu, Z.G. Zhu, Y. Feng, and J.P. Shui, J. Phys. Condens. Matter **13**, 11435 (2001).

[3] K.Q. Lu, Q. Wang, C. Li, Y. Wang, and X. Chen, J. Non-Cryst. Solids **312–314**, 34 (2002).

[4] U. Dahlborg, M. Calvo-Dahlborg, P.S. Popel, and V.E. Sidorov, Eur. Phys. J **B14**, 639 (2000).

[5] X.F. Li, F.Q. Zu, L.J. Liu, J. Yu, and B. Zhou, Phys. Chem. Liquid **45**, 531 (2007).

[6] T. Iida and R.I.L. Guthrie, *The Properties of Liquid Metals* (Clarendon Press, Oxford, 1993).

[7] N.K.P. Singh, R.N. Singh, and P.B. Choudhary, J. Phys. Condens. Matter **3**, 3635 (1991).

[8] H. Reichert, O. Klein, H. Dosch, M. Denk, V. Honkimaki, T. Lippamnn, and G. Reiter, Nature **408**, 839 (2000).

[9] W. Van der Lugt, J. Phys. Condens. Matter **8**, 6115 (1996).

[10] W. Jank and J. Hafner, J. Non-Crystall. Solids **114**, 16 (1989).

[11] T. Itami, S. Munejiri, T. Masaki, H. Aoki, Y. Ishii, T. Kamiyama, Y. Senda, F. Shimojo, and K. Hoshino, Phys. Rev **B67**, 064201 (2003).

[12] Y. Waseda, *The Structure of Non-Crystalline Materials* (McGraw-Hill, New York, 1980).

[13] T.B. Massalski, *Binary Alloy Phase Diagram* (American Society for Metals, Metals Park, Ohio, 1986).

[14] L. Noren, R.L. Withers, S. Schmid, F.J. Brink, and T.V. Old, J. Solid State Chem. **179**, 404 (2006).

[15] V. Vassiliev, M. Lelaurain, and J. Hertz, J. Alloys Compd. **247**, 223 (1997).